32nd URSI GASS, Montreal, 19–26 August 2017

The effect of the ionosphere on astronomical observations below 100 MHz

F. de Gasperin*(1), M. Mevius(2), and H. Intema(1)
(1) Leiden Observatory, Leiden University, P.O.Box 9513, NL-2300 RA, Leiden, The Netherlands
(2) ASTRON, P.O.Box 2, NL-7990 AA, Dwingeloo, the Netherlands

Abstract

We derive the expected systematic error induced by the ionosphere on radio astronomical observations at low frequencies. We compare our predictions with data from the Low Frequency Array (LOFAR). We show that the systematic errors on the phases of the instrument can be described as a sum of four effects (clock, ionosphere 1st, 2nd, and 3rd order). We show that the ionosphere corrupts also the recorded data amplitude through scintillations. Finally, we report values of the ionosphere structure function in line with the literature.

1 Introduction

LOFAR [8] is a radio interferometer that operates at very low frequencies ($10-240$ MHz). It has 38 stations (aperture arrays capable of multi-beam forming) in the Netherlands, divided in 24 "core stations", concentrated within 4 km, and 14 "remote stations", providing baselines up to ~ 120 km[1]. Thirteen "international stations" are spread across Europe, but they will not be considered in this paper. LOFAR uses two antenna types: High Band Antenna (HBA, used to observe in the frequency range $110-240$ MHz) and Low Band Antenna (LBA, used to observe in the frequency range $10-90$ MHz). In this paper we will consider only data from the LBA system, that is the most heavily affected by ionospheric systematic errors.

The ionisation of the ionosphere happens during the day and is balanced by recombination at night. The peak of the free electron density is at a height of ~ 300 km. The free electron column density along a line of sight (LoS) through the ionosphere is generally referred to as the total electron content (TEC). The TEC unit (TECU) is 10^{16} m^{-2}, which is a typically observed value at zenith during nighttime. The refraction and propagation delay are caused by a varying refractive index n of the ionospheric plasma along the wave trajectory. The total propagation delay, integrated along the LoS at frequency ν, results in a phase rotation given by

$$\Phi^{\rm ion} = -\frac{2\pi\nu}{c}\int_{\rm LoS}(n-1)\,{\rm d}l \qquad (1)$$

[1]An updated outline of LOFAR station positions is available at http://www.astron.nl/ heald/lofarStatusMap.html

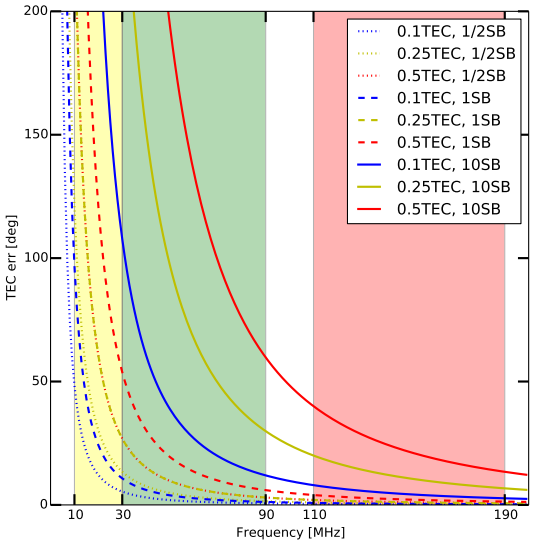

Figure 1. Ionospheric-induced phase variation between the beginning and the end of a band of 1/2, 1 and 10 LOFAR sub bands (SB; 1 SB = 0.2 MHz). The dTEC is assumed to be 0.1, 0.2 and 0.5 TECU. These are typical values for distances of a few tens of km. A phase variation larger than $\sim 100^\circ$ creates strong decorrelation. This plot shows the maximum amount of average (or the maximum band usable to find a single solution) before decorrelating the signal. Coloured bands are the frequency ranges observed by LOFAR.

Neglecting the frictional force and assuming a cold, collisionless, magnetised plasma (such as the ionosphere), the refractive index n can be calculated exactly [2]. For signals with frequencies $\nu \gg \nu_p$ (the plasma frequency, that for the ionosphere is around $1-10$ MHz), it can be expanded (see e.g. [1]) into a second-order Taylor approximation retaining only terms up to ν^{-4}:

$$n = 1 - \frac{q^2}{8\pi^2 m_e \varepsilon_0}\cdot\frac{n_e}{\nu^2} \pm \frac{q^3}{16\pi^3 m_e^2 \varepsilon_0}\cdot\frac{n_e B\cos\theta}{\nu^3} - \frac{q^4}{128\pi^4 m_e^2 \varepsilon_0^2}\cdot\frac{n_e^2}{\nu^4} - \frac{q^4}{64\pi^4 m_e^3 \varepsilon_0}\cdot\frac{n_e B^2(1+\cos^2\theta)}{\nu^4}, \qquad (2)$$

where n_e: number density of free electrons, B: magnetic field strength, θ is the angle between the magnetic field

dTEC (TECU)	I ord 30 MHz	II ord (day/night) 30 MHz	I ord 60 MHz	II ord (day/night) 60 MHz	I ord 150 MHz	II ord (day/night) 150 MHz
0.5 (remote st., bad iono.)	8067	294 / 214	4033	73 / 50	1613	12 / 8
0.1 (remote st., good iono.)	1613	126 / 46	806	31 / 10	322	5 / 2
0.03 (across FoV)	404	97 / 16	242	24 / 4	96	4 / < 1
0.01 (core st.)	160	88 / 8	80	22 / 2	31	4 / < 1

Table 1. Ionospheric phase errors in degrees

$\vec{B}$ and the electromagnetic wave propagation direction, q: electron charge, m_e: electron mass, ε_0: electric permittivity in vacuum. In red the parameters driven by ionospheric conditions. The first term is associated with a delay proportional to the TEC along the LoS. This is the dominant term, for most radio-astronomical applications at frequencies higher than a few hundreds of MHz higher order terms can be ignored. The second term is related to Faraday rotation, the positive sign is associated with left hand polarised signals and the negative sign with right hand polarised signals. This term depends on TEC and Earth's magnetic field. The last two terms are usually ignored but can become relevant for observations at very low frequencies (< 50 MHz), the first is dominant and depend on the distribution of the electrons in the ionosphere. The term is larger if ionosphere electrons are concentrated in thin layers and not uniformly distributed.

By using Eq. 2 we can give an order of magnitude estimation of the expected effect of 1st and 2nd orders (see also [3], chapter 9):

$$\begin{aligned} \delta\Phi_1 &= -8067\left(\frac{\nu}{60\text{MHz}}\right)^{-1}\left(\frac{\delta\text{TEC}}{1\text{TECU}}\right)\text{[deg]};\\ \delta\Phi_2 &= \pm 105\left(\frac{\nu}{60\text{MHz}}\right)^{-2}\left[\left(\frac{\delta\text{TEC}}{1\text{TECU}}\right)\right. \\ &\left. + \left(\frac{\text{TEC}}{1\text{TECU}}\right)\cdot\left(\frac{\delta\text{B}}{40\mu\text{T}}\right)\right]\text{[deg]}; \end{aligned} \quad (3)$$

Where we assumed a magnetic field $B = 40\mu$T with $\theta = 45^\circ$. Total TEC can vary from ~ 1 to ~ 20 from night to day respectively and influences the second order term. Considering a differential TEC (dTEC) of $\simeq 0.3$ TECU, which is a plausible number for baselines ~ 50 km (see Fig. 3), and observing at 60 MHz, the first order term produces phase variations of several complete phase cycles. The Faraday rotation instead produces an effect of around $\pm 30^\circ/50^\circ$ (with different sign for the two polarisations) at night/day assuming $\delta B = 1\%$. This effect is not negligible and needs to be corrected. The effect quickly becomes more severe at lower frequencies because of the $1/\nu^2$ dependency. Higher order effects can be ignored. However, at very low frequency (~ 20 MHz) the third order effect can produce large phase errors and could become problematic. More examples are given in Table 1.

2 Data

We used a LOFAR LBA ($22-70$ MHz) observation pointed at 3C196 and obtained on March, 1st 2013 ($17:00 \rightarrow 23:00$). The dataset has been calibrated using procedures that will be described in de Gasperin et al. (2017, in prep.). Here we will focus on the outcome of the calibration to describe the influence of the ionosphere on the signal measured by the antennas. For each station pair, radio interferometers record streams of data, called visibilities. While ionospheric effects are clearly present in the visibilities, it is easier to analyse them by looking at solutions, i.e. station-based complex gain factors derived when observing a source with a known position and flux density.

Because of the low antenna sensitivity and the high sky temperature the LOFAR LBA system is often in a low signal to noise ratio regime. A common way to compensate for this is to include longer time intervals when finding solutions. At low frequencies this becomes a trade-off between signal to noise and decorrelation. The ionosphere tends to vary very quickly and averaging over more than ~ 5 s often does not allow for these changes to be tracked. Furthermore, combining too many frequency channels is also not advisable. As shown in Fig. 1, between the edges of a single LOFAR subband (1 SB = 0.2 MHz) centred at 30 MHz, there is a differential phase of 50° (assuming two stations with a dTEC of 0.5 TECU). For compact arrays (baselines shorter than a few km, with dTEC $\lesssim 0.1$ TECU), this constraint can be relaxed.

Most of the systematic effects described in this paper are direction dependent. This means that the effects vary strongly as a function of viewing direction, even across the field of view of the telescope. These type of systematic errors are particularly problematic to solve as they require either simultaneous estimation in multiple directions or an iterative approach like "peeling" [7].

3 Systematic effects

Dispersive delay In Fig. 2 we show phase solutions for each station for the 6 hr of observation, in the frequency range $22-70$ MHz. All stations labelled CS are "core stations" — these stations share the same clock and are close together. Stations labelled RS are "remote stations" and they have each an independent clock. Clocks are not perfectly synchronised and they might drift in time with respect to each other. This imprints a time-variable system-

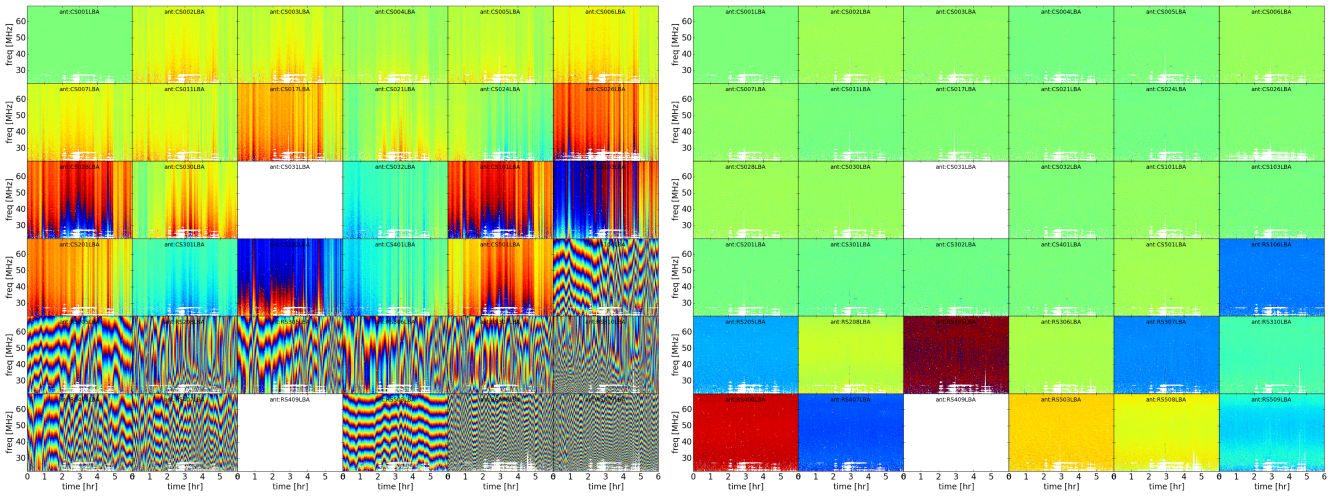

Figure 2. Gain phase solutions (from $+\pi$: blue to $-\pi$: red) for the RR polarisation. Each panel is one station. White pixels represents bad data that were removed, stations CS 031 and RS 409 were fully removed due to hardware issues and strong radio frequency interference (RFI) contamination, respectively. In the right panel we show the residuals after subtracting all the effects shown in Fig. 3.

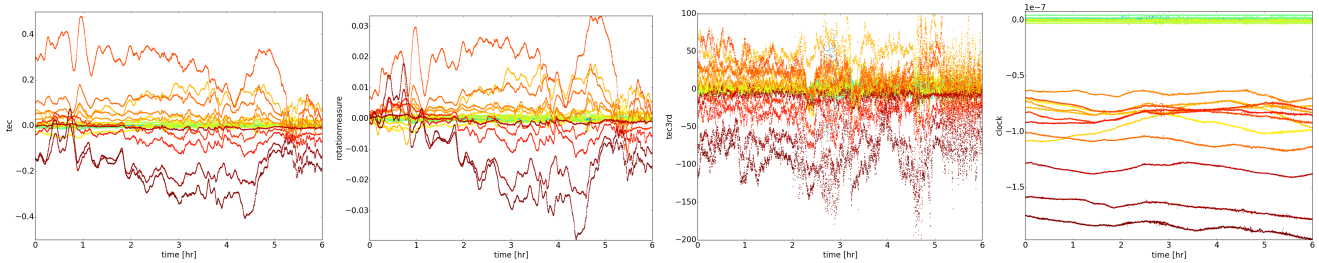

Figure 3. Left to right: total electron content variation along the observation (in TECU). Faraday rotation (in rad). Ionospheric 3rd order effect (in arbitrary units). Instrumental clock delay (in s). All values are differential between CS 001 (assumed constant at 0) and all other stations (from blue to red in alphabetical order).

atic error on the phases of remote stations which is linear in ν. This effect dominates the phase error in the closest remote stations such as RS106 (uniform phase wrapping). In the most distant remote stations (such as RS508 or RS509) the $1/\nu$ effect of the ionosphere dominates (phases wraps faster on the lower part of the plots). We can use the different frequency dependency of the two effects to disentangle their contribution [9].

In Fig. 3 the clock and the ionospheric delay are separated and plotted for each station. All plots shows differential effects with respect to core station CS001. As a consequence, nearby core stations have very small dTEC and a constant differential clock (due to an unknown instrumental delay). Conversely, remote stations show dTEC values up to 0.5 TECU for stations that are around 50 km away from CS001. Furthermore, a clear correlation between stations located nearby is also visible (e.g. RS508, RS509 are the two bottom lines of the plot).

Higher order terms With this dataset we were able to measure the second order ionospheric effect due to Faraday rotation. To estimate this effect we took advantage of its different sign in the right and left polarisations (see Eq. 2). This required a conversion of the dataset from linear to circular polarisation. We then fitted a differential delay between the two polarisations with a $1/\nu^2$ dependency. In Fig. 3 we show the result in terms of rotation measure ($\Phi = \mathrm{RM}\lambda^2$).

Again we notice that nearby stations have similar behaviour and that there is also a correlation between the dTEC and the RM. This is a consequence of the presence of n_e in both the first and second terms of Eq. 2. The measured RM of 0.03 rad produces $\sim 45^\circ$ phase error, which is compatible with expectations given a measured dTEC of 0.3 TECU.

Amplitude scintillations Scintillations are caused by electromagnetic waves scattered in a non uniform medium with small changes in the refractive index such as the ionosphere. A plane wave that enters such a medium with a spatially uniform phase, exits the medium with a spatially irregular phase. After propagation to a station, the irregular phases may combine either constructively or destruc-

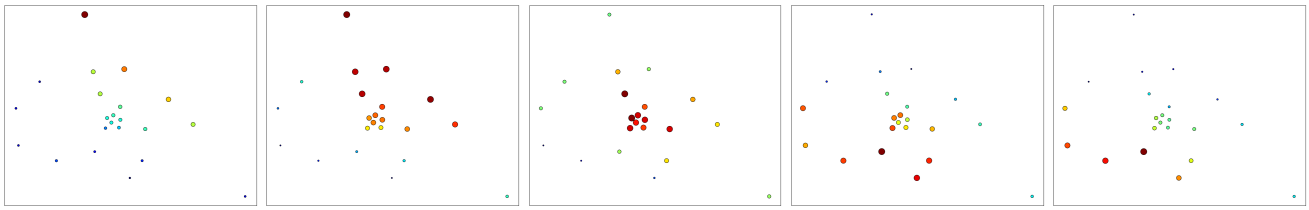

Figure 4. Top to bottom: time evolution of amplitude solutions for LOFAR core stations. Each point represent a core station an it is positioned in the plot according to its geographical location. Colour (blue to red) and size (small to large) are related with the value of the amplitude correction. A wave travelling north south is visible.

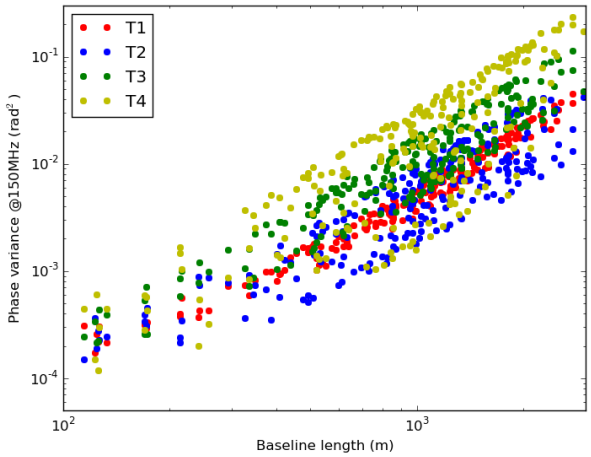

Figure 5. Phase structure function divided into four time chunks. The last part of the observations is visibly more affected by ionospheric disturbances also in Fig. 3. The phase variance is converted to the expected value at 150 MHz to compare it with other experiments such as HBA LOFAR and MWA.

tively (see [4]). As a consequence, the wave amplitude is increased or decreased and the gain amplitude solutions of the station compensate the effect by producing an exact opposite trend. At frequencies below 100 MHz, scintillations are always present in LOFAR solutions to some degree.

An example of this is visible in Fig. 4, where an "amplitude wave" crosses the core area (4 km) in 1 minute, therefore travelling at a velocity of ~ 240 km/h. Projecting half of the linear size of the wave to the height of 300 km we can estimate an angular size over which amplitude corrections can be considered fairly uniform, which is $\sim 20'$. Scintillations therefore create a direction-dependent amplitude effects across the field-of-view.

4 Structure function

We divided the observations into three time chunks and calculated the ionosphere phase structure function as described in [5]. For Kolmogorov turbulence, the phase structure function is a power-law of the form:

$$D(r) = \left(\frac{r}{r_{\rm diff}}\right)^{\beta}. \quad (4)$$

We fit this function to the data to obtain an estimation of β (expected to be $5/3 = 1.67$ for pure Kolmogorov turbulence) and of $r_{\rm diff}$, the spatial scale over which the phase variance is 1 rad^2, and is referred to as the diffractive scale [6]. We obtained $\beta = 1.7, 1.6, 1.8, 1.9$ and $r_{\rm diff@150MHz} = 14.8, 19.1, 9.5, 6.5$ km, for time chunks 1 to 4 respectively (see Fig. 5).

Once removed the large ionospheric gradient (e.g. with a direction independent calibration), higher orders of the refractive index expansion in Eq. 2 can be small enough to be considered uniform across the LOFAR beam. To test this hypothesis we can use the structure function. The LOFAR primary beam size is $\sim 4^\circ$, that corresponds to 20 km at a 300 km high ionospheric layer. With a diffractive scale of 10 km and assuming $\beta = 1.7$, Eq. 4 gives a phase variance of ~ 3 rad^2 at 150 MHz. This corresponds to a dTEC of about 0.03 TECU. Consequently, even at 60 MHz, only the first order term changes substantially across the FoV while other terms can be considered constant.

References

[1] Datta-Barua S. et al. (2008), Radio Science, 43, RS5010

[2] Davies K. (1990) Ionospheric Radio, IEE Electromagnetic Waves 31, Peter Pergrinus Ltd., London, UK.

[3] Petit G. and Luzum B. (2010) IERS Technical Note 36, Frankfurt am Main: Verlag des Bundesamts für Kartographie und Geodäsie, ISBN 3-89888-989-6

[4] Kintner et al. (2007) Space weather, 5, S09003

[5] Mevius M. et al. (2016) Radio Science, 51, 927-941

[6] Narayan R. (1992), Philosophical Transactions: Physical Sciences and Engineering, 341, 1660, 151-165

[7] Noordam, J. E. (2004) Proceedings of SPIE, 5489, 817-825

[8] van Haarlem, M. P. et al. (2013) Astronomy & Astrophysics, 556, A2

[9] van Weeren, R. J. et al. (2016) The Astrophysical Journal Supplement Series, 223, id2